

# On the distributed resistor-constant phase element transmission line in a reflective bounded domain

Anis Allagui\*\*

*Dept. of Sustainable and Renewable Energy Engineering,  
University of Sharjah, Sharjah, P.O. Box 27272, United Arab Emirates<sup>†</sup> and  
Dept. of Electrical and Computer Engineering, Florida International University, Miami, FL33174, United States*

Enrique H. Balaguera

*Escuela Superior de Ciencias Experimentales y Tecnología,  
Universidad Rey Juan Carlos, C/ Tulipán, s/n, 28933 Móstoles, Madrid, Spain*

Chunlei Wang

*Dept. of Mechanical and Aerospace Engineering, University of Miami, FL, United States*

In this work we derive and study the analytical solution of the voltage and current diffusion equation for the case of a finite-length resistor-constant phase element (CPE) transmission line (TL) circuit that can represent a model for porous electrodes in the absence of any Faradic processes. The energy storage component is considered to be an elemental CPE per unit length of impedance  $z_c(s) = 1/(c_\alpha s^\alpha)$  instead of the ideal capacitor usually assumed in TL modeling. The problem becomes a time-fractional diffusion equation that we solve under galvanostatic charging, and derive from it a reduced impedance function of the form  $z_\alpha(s_n) = s_n^{-\alpha/2} \coth(s_n^{\alpha/2})$ , where  $s_n = j\omega_n$  is a normalized frequency. We also derive the system's step response, and the distribution function of relaxation times associated with it.

## I. INTRODUCTION

The reduced impedance model given by  $z(s_n) = s_n^{-1/2} \coth(s_n^{1/2})$ , where  $s_n = j\omega_n$  is a normalized angular frequency, is known as the reflective finite-length Warburg impedance that represents the linear diffusion dynamics in restricted thin electrodes [1–4]. It has been introduced by Franceschetti and MacDonald [5] to describe the case of diffusion of gas or metal species through a metallic electrode or along the electrode/electrolyte interface, and by Gabrielli et al. [6] to describe reactions on polymer film coated electrodes. It can be shown that this diffusion impedance transitions from that of the Warburg element at high frequencies, scaling as  $s_n^{-1/2}$ , to that of a resistance in series with a capacitance at low frequencies [6]. However, experimental evidence shows clear deviations from these characteristic features [2, 6–10]. Cabanel et al. [11] proposed a variant of the restricted diffusion impedance function by introducing empirically a dispersion coefficient  $\alpha$  ( $0 < \alpha < 1$ ) in the function so that it takes the form:  $s_n^{-\alpha/2} \coth(s_n^{\alpha/2})$ . This model has since been applied to the study of a multitude of electrochemical systems, such as the diffusion of H in a thin layer of  $H_x\text{Nb}_2\text{O}_5$  [11], lithium-ion batteries [12], supercapacitors [10], etc.

As an example, we show in Fig. 1 the Nyquist impedance plot of a NEC/Tokin supercapacitor, model

FG Series, rated 5.5 V, 1.0 F (part num. FG0H105ZF). The device was first maintained at a constant voltage of 2.7 V for 5 min to avoid undesired transient variations in its electrical response, and then subjected to a 10 mV rms stepping sine excitation from the frequency of 1 MHz down to 10 mHz. We recorded impedance data at 10 frequency points per decade. Complex nonlinear least squares fitting of the very low frequency branch from 10 to 20 mHz (i.e. from point (20.59, 22.09) Ohm to point (19.75, 12.24) Ohm) with a model consisting of a resistance in series with a constant phase element (CPE), i.e. of impedance:

$$Z_l(f) = R_s + \frac{1}{C_\alpha (i2\pi f)^\alpha} \quad (1)$$

gives the line indicated in red color in in Fig. 1(a). This line is inclined with an angle of 83 deg. vs. the real axis, which corresponds to an  $\alpha$ -value of 0.92 in Eq. 1. The values of the series resistance and pseudocapacitance are found to be 18.0 Ohm and  $0.56 \text{ F s}^{\alpha-1}$ , respectively. Whereas the other inclined line in the figure (in orange color) fitting the impedance data spanning the frequency range from 65 mHz to 35 Hz is inclined with an angle of 40 deg., i.e.  $\alpha = 0.45$ , which is practically half of the  $\alpha$ -value for the low frequency segment of data. Here the series resistance and pseudocapacitance are found to be 10.8 Ohm and  $0.16 \text{ F s}^{\alpha-1}$ , respectively. Now fitting the low- and high-frequency impedance data together from 10 mHz to 35 Hz with the dimensional model corresponding to Eq. 42, i.e.:

$$Z_{\text{TL}}(f) = R_s + R_d \frac{\coth((i2\pi f \tau)^{\alpha/2})}{(i2\pi f \tau)^{\alpha/2}} \quad (2)$$

\* aallagui@sharjah.ac.ae

<sup>†</sup> Also at Center for Advanced Materials Research, Research Institute of Sciences and Engineering, University of Sharjah, Sharjah, P.O. Box 27272, United Arab Emirates

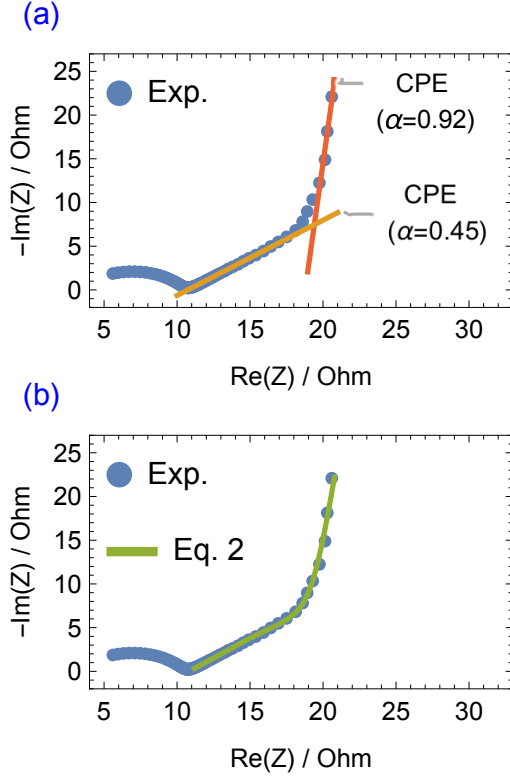


FIG. 1. Nyquist plot of experimental impedance data measured for a NEC/Tokin supercapacitor device on a Biologic VSP-300 electrochemical station from 1 MHz down to 10 mHz with  $V_{ac} = 10$  mV rms. In solid lines we show fitting of the impedance data with the models given by Eqs. 1 (the two straight lines in (a)) and 2 (green line in (b))

gives the parameters set:  $R_s = 10.8$  Ohm,  $R_d = 24.2$  Ohm,  $\tau = 17.8$  s, and  $\alpha = 0.94$ . As one can appreciate from Fig. 1(b), the curved impedance data are nicely fitted with this model. We note that the value of the parameter  $\alpha$  obtained from Eq. 2 is practically equal to that obtained from fitting the low frequency branch of impedance using the  $R_s$ -CPE model (Eq. 1).

In this study, we demonstrate that this modified impedance function can be derived from the anomalous time-fractional diffusion equation representing a distributed  $R$ -CPE transmission line (TL) in a bounded one-dimensional domain (Eq. 8 below). We recall that in a single pore of an electrified porous electrode filled with electrolyte, the electrolyte's resistance and the electrolyte-electrode interface double-layer capacitance can be viewed respectively as a distributed resistance and distributed capacitance over the the length of the pore [13]. This equivalent ladder-like circuit model can be represented by cutting up the overall resistance and capacitance, and connecting the building blocks in a TL circuit (Fig. 2). In the limit of infinitely many infinitesimally small self-similar circuit elements connected together, the potential drop across the capacitors of the

TL circuit can be modeled by a diffusion-type partial differential equation [14]. That is:

$$\frac{\partial v(x, t)}{\partial t} = \frac{1}{rc} \frac{\partial^2 v(x, t)}{\partial x^2}, \quad 0 < x < \infty, t \geq 0 \quad (3)$$

where  $r$  and  $c$  represent respectively constant resistance/capacitance per unit length of the TL.

In a recent contribution by some of the co-authors [15], this problem of diffusion has been generalized and studied for the case of a CPE acting as the capacitive energy storage element instead of an ideal capacitor. This is to account more generally for the anomalous resistive-capacitive behavior observed in both frequency and time-domain data on most porous electrodes used in practical applications (supercapacitors, fuel cells, batteries, etc.). The current on the CPE is given by the fractional-order differential equation:

$$i_c(x, t) = C_\alpha {}_0D_t^\alpha v_c(x, t) \quad (4)$$

where  $C_\alpha$  is a pseudocapacitance in units of  $F s^{\alpha-1}$ , and  ${}_0D_t^\alpha$  is the Caputo differential operator of order  $\alpha$  ( $0 < \alpha \leq 1$ ) defined as:

$${}_0D_t^\alpha f(t) := \frac{1}{\Gamma(m-\alpha)} \int_0^t (t-\tau)^{m-\alpha-1} f^{(m)}(\tau) d\tau \quad (5)$$

Here  $m \in \mathbb{N}$ ,  $m-1 < \alpha < m$  ( $m = 1$  in our case),  $\Gamma(z) = \int_0^\infty u^{z-1} e^{-u} du$ , ( $\text{Re}(z) > 0$ ) is the gamma function, and  $f^{(m)}(t) = d^m f(t)/dt^m$  is the  $m^{\text{th}}$  derivative of  $f(t)$  with respect to  $t$ . This leads in the frequency domain to the impedance of the CPE being [16–21]:

$$Z_c(s) = \frac{1}{C_\alpha s^\alpha} \quad (6)$$

( $s = j\omega$ ) which simplifies to that of an ideal capacitor when  $\alpha = 1$ . The problem of anomalous diffusion for the case of a semi-infinite  $R$ -CPE TL circuit becomes:

$${}_0D_t^\alpha v(x, t) = \frac{1}{rc_\alpha} \frac{\partial^2 v(x, t)}{\partial x^2}, \quad 0 < x < \infty, t \geq 0 \quad (7)$$

where  $r$  and  $c_\alpha$  represent again a constant resistance/pseudo-capacitance per unit length (replace  $c$  with  $c_\alpha$  in Fig. 2). The solution obtained for Eq. 7 in response to a step voltage at  $x = 0$  and assuming zero current at infinity has been derived using the Laplace transform method, and provided in terms of the Fox's  $H$ -function [15]. We also derived the total impedance of the modified TL circuit, and found that the system itself behaves as a CPE of half the order of that of the constituting CPEs ( $Z_{\text{TL}}(s) = \sqrt{r/c_\alpha} s^{-\alpha/2}$ ). This can be viewed as a generalization of the Warburg semi-infinite diffusion along  $RC$ -based TL, which is known to lead to an equivalent CPE of order 0.5 [22].

Here, we focus on the solution of the same time-fractional diffusion along a self-similar  $R$ -CPE TL circuit, but instead on a bounded one-dimensional domain [0;  $L$ ]

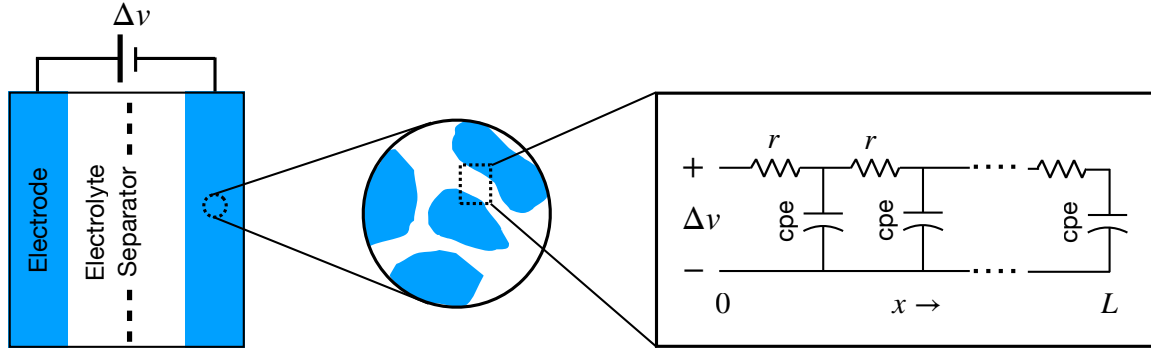


FIG. 2. Schematic of an electrified pore of a porous electrode in contact with an electrolyte modeled by a finite-length  $R$ -CPE transmission line model.

(Fig. 2). The motivation is that in porous electrodes in contact with an electrolyte in electrochemical devices such as supercapacitors, batteries, capacitive desalination modules and electrochemical (bio)sensors [14, 23–25], the generalized TL diffusion equation on a finite interval is in practice more relevant to the study of their responses [3]. We make use of combined transforms using the finite Fourier cosine transform on the spatial variable and the Laplace transform on the time variable in the diffusion equation [26]. The voltage drop is found as an infinite series of the Mittag-Leffler function or the Fox's  $H$ -function. We also derive the impedance function of the circuit and found it to be indeed in the desired form of  $s_n^{-\alpha/2} \coth(s_n^{\alpha/2})$ . From this impedance we derive by inverse Laplace transform the system's step response, and by another iteration of inverse Laplace transform the distribution function of relaxation times of the Debye type associated with it.

## II. THEORY

### A. Statement of anomalous diffusion problem

We consider in this study the time-fractional partial differential equation (PDE) of 1D diffusion over the bounded domain  $[0; L]$ :

$${}_0D_t^\alpha v(x, t) = \frac{1}{rc_\alpha} \frac{\partial^2 v(x, t)}{\partial x^2}, \quad 0 < x < L, \quad t > 0 \quad (8)$$

Furthermore, we consider the following boundary conditions [27]:

$$-\frac{1}{r_0} \left( \frac{\partial v(x, t)}{\partial x} \right)_{x=0} = i_0, \quad t > 0 \quad (9)$$

$$\left( \frac{\partial v(x, t)}{\partial x} \right)_{x=L} = 0, \quad t > 0 \quad (10)$$

where  $i_0$  is a constant current, and the initial condition:

$$v(x, t=0) = 0, \quad 0 < x < L \quad (11)$$

Again, this TL model describes the case of galvanostatic charging of a uniform and homogeneous pore in a porous conductive material completely filled with an electrolyte, where the capacitive behavior is represented by a CPE of constant parameters (Fig. 2).

### B. Solution by operational method

We first apply the finite Fourier cosine transform to both sides of Eq. 8 with respect to the variable  $x$ . The finite Fourier cosine transform is defined for a function  $f(x)$  in the interval  $[0; L]$  as [28–30]

$$\bar{f}(k) = \mathcal{F}_c[f(x); k] = \int_0^L f(x) \cos(k\pi x/L) dx \quad (12)$$

where  $k = 1, 2, \dots$ . This is derived from the Fourier cosine series for  $f(x)$ :

$$f(x) = \frac{a_0}{2} + \sum_{k=1}^{\infty} a_n \cos(k\pi x/L) \quad (13)$$

After taking into account the boundary conditions, the transformed equation becomes:

$${}_0D_t^\alpha \bar{v}(k, t) + \frac{(k\pi/L)^2}{rc_\alpha} \bar{v}(k, t) - \frac{r_0 i_0}{rc_\alpha} = 0 \quad (14)$$

We carry on by taking the Laplace transform defined for a function  $f(t)$  ( $t > 0$ ) as

$$\tilde{f}(s) = \mathcal{L}\{f(t); s\} = \int_0^{\infty} e^{-st} f(t) dt, \quad \text{Re}(s) > 0 \quad (15)$$

of both sides of Eq. 14 with respect to  $t$ , which leads to the diffusion equation in the  $(k, s)$ -domain to be:

$$\tilde{v}(k, s) = \frac{r_0 i_0}{rc_\alpha} \frac{s^{-1}}{s^\alpha + (k\pi/L)^2/(rc_\alpha)} \quad (16)$$

We recall that the Laplace transform of the Caputo time-fractional derivative of order  $\alpha$  is given by:

$$\mathcal{L} [{}_0D_t^\alpha f(t); s] = s^\alpha \tilde{f}(s) - \sum_{k=0}^{m-1} s^{\alpha-k-1} f^{(k)}(0^+) \quad (17)$$

Now for the inversion steps, we start first by applying the inverse Laplace transform defined as:

$$f(t) = \mathcal{L}^{-1}\{\tilde{f}(s); t\} = \frac{1}{2\pi i} \int_{\gamma-i\infty}^{\gamma+i\infty} e^{st} \tilde{f}(s) ds \quad (18)$$

We use the Prabhakar formula [31]:

$$\mathcal{L}^{-1} \left\{ \frac{s^{\beta-1}}{s^\alpha + a}; t \right\} = t^{\alpha-\beta} E_{\alpha, \alpha-\beta+1}(-at^\alpha) \quad (19)$$

where  $E_{a,b}(z)$  is the Mittag-Leffler function and  $\text{Re}(\alpha - \beta) > -1$ . Recall that the three-parameter Mittag-Leffler function is defined as:

$$E_{a,b}^c(z) := \sum_{k=0}^{\infty} \frac{(c)_k}{\Gamma(ak+b)} \frac{z^k}{k!} \quad (a, b, c \in \mathbb{C}, \text{Re}(a) > 0) \quad (20)$$

with  $(c)_k = c(c+1) \dots (c+k-1) = \Gamma(c+k)/\Gamma(c)$ . Thus, we obtain from this inversion step:

$$\bar{v}(k, t) = \frac{r_0 i_0}{rc_\alpha} t^\alpha E_{\alpha, \alpha+1} \left( -\frac{(k\pi/L)^2 t^\alpha}{rc_\alpha} \right) \quad (21)$$

$$= \frac{r_0 i_0}{(k\pi/L)^2} \left[ 1 - E_\alpha \left( -\frac{(k\pi/L)^2 t^\alpha}{rc_\alpha} \right) \right] \quad (22)$$

$$= \frac{r_0 i_0}{(k\pi/L)^2} H_{1,2}^{1,1} \left[ \frac{(k\pi/L)^2 t^\alpha}{rc_\alpha} \middle| \begin{matrix} (1, 1) \\ (1, 1), (0, \alpha) \end{matrix} \right] \quad (23)$$

We recall here that the  $H$ -function of order  $(m, n, p, q) \in \mathbb{N}^4$ ,  $(0 \leq n \leq p, 1 \leq m \leq q)$  and with parameters  $A_j \in \mathbb{R}_+$  ( $j = 1, \dots, p$ ),  $B_j \in \mathbb{R}_+$  ( $j = 1, \dots, q$ ),  $a_j \in \mathbb{C}$  ( $j = 1, \dots, p$ ) and  $b_j \in \mathbb{C}$  ( $j = 1, \dots, q$ ) is defined for  $z \in \mathbb{C}$ ,  $z \neq 0$  by the Mellin-Barnes integral [32]:

$$H_{p,q}^{m,n} \left[ z \middle| \begin{matrix} (a_1, A_1), \dots, (a_p, A_p) \\ (b_1, B_1), \dots, (b_q, B_q) \end{matrix} \right] = \frac{1}{2\pi i} \int_L h(s) z^{-s} ds \quad (24)$$

where:

$$h(s) = \frac{\prod_{j=1}^m \Gamma(b_j + B_j s) \prod_{j=1}^n \Gamma(1 - a_j - A_j s)}{\prod_{j=m+1}^q \Gamma(1 - b_j - B_j s) \prod_{j=n+1}^p \Gamma(a_j + A_j s)}$$

$$z^{-s} = \exp[-s(\ln|z| + i \arg z)]$$

with  $\arg z$  taking any real value. The contour of integration  $L$  is a suitable contour separating the poles of  $\Gamma(b_j + B_j s)$  ( $j = 1, \dots, m$ ) from the poles of  $\Gamma(1 - a_j -$

$A_j s)$  ( $j = 1, \dots, n$ ). An empty product is always interpreted as unity.

Then, by inverse finite Fourier cosine transform defined as:

$$f(x) = \mathcal{F}_c^{-1}[\bar{f}(k); x] = \frac{1}{L} \bar{f}(0) + \frac{2}{L} \sum_{k=1}^{\infty} \bar{f}(k) \cos(k\pi x/L) \quad (25)$$

we obtain the voltage  $v(x, t)$  as the infinite series:

$$v(x, t) = \frac{r_0 i_0}{rc_\alpha L} \frac{t^\alpha}{\Gamma(1+\alpha)} + \frac{2r_0 i_0}{L} \sum_{k=1}^{\infty} \frac{\cos(k\pi x/L)}{(k\pi/L)^2} H_{1,2}^{1,1} \left[ \frac{(k\pi/L)^2 t^\alpha}{rc_\alpha} \middle| \begin{matrix} (1, 1) \\ (1, 1), (0, \alpha) \end{matrix} \right] \quad (26)$$

which can also be expressed in terms of the Mittag-Leffler function using Eq. 21, as shown also by Luchko using the method of separation of variables [33, 34]. For  $\alpha = 1$  reduces to the ideal  $RC$ -based TL case [27]:

$$v(x, t) = \frac{r_0 i_0 t}{rcL} + \frac{2r_0 i_0}{L} \sum_{k=1}^{\infty} \frac{\cos(k\pi x/L)}{(k\pi/L)^2} \left[ 1 - \exp\left(-\frac{(k\pi/L)^2 t}{rc}\right) \right] \quad (27)$$

Note that by inverse Fourier cosine transform defined as:

$$f(x) = \mathcal{F}_s^{-1}[\bar{f}(\omega_k); x] = \frac{2}{\pi} \int_0^{\infty} \bar{f}(\omega_k) \cos(\omega_k x) d\omega_n \quad (28)$$

where  $\omega_k = k\pi/L$  in our case, and using the integral formula [32]:

$$\int_0^{\infty} x^{\rho-1} \cos(ax) H_{p,q}^{m,n} \left[ bx^\sigma \middle| \begin{matrix} (a_p, A_p) \\ (b_q, B_q) \end{matrix} \right] dx = \frac{2^{\rho-1} \sqrt{\pi}}{a^\rho} H_{p+2,q}^{m,n+1} \left[ b \left( \frac{2}{a} \right)^\sigma \middle| \begin{matrix} (\frac{2-\rho}{2}, \frac{\sigma}{2}) \\ (b_q, B_q) \end{matrix}, (a_p, A_p), (\frac{1-\rho}{2}, \frac{\sigma}{2}) \right] \quad (29)$$

(with  $\rho = -1$ ,  $b = t^\alpha/(rc_\alpha)$ ,  $\sigma = 2$ ) we obtain the voltage as:

$$v(x, t) = \frac{2r_0 i_0}{\pi} \int_0^{\infty} \frac{\cos(\omega_k x)}{\omega_k^2} H_{1,2}^{1,1} \left[ \frac{\omega_n^2 t^\alpha}{rc_\alpha} \middle| \begin{matrix} (1, 1) \\ (1, 1), (0, \alpha) \end{matrix} \right] d\omega_n \quad (30)$$

$$= \frac{r_0 i_0 x}{2\sqrt{\pi}} H_{2,1}^{0,2} \left[ \frac{4t^\alpha}{rc_\alpha x^2} \middle| \begin{matrix} (1, 1), (3/2, 1) \\ (0, \alpha) \end{matrix} \right] \quad (31)$$

$$= \frac{r_0 i_0 x}{2\sqrt{\pi}} H_{1,2}^{2,0} \left[ \frac{rc_\alpha x^2}{4t^\alpha} \middle| \begin{matrix} (1, \alpha) \\ (0, 1), (-1/2, 1) \end{matrix} \right] \quad (32)$$

$$= \frac{r_0 i_0 x}{2\sqrt{\pi}} H_{1,2}^{2,0} \left[ (4\text{Fo}_x) \middle| \begin{matrix} (1, \alpha) \\ (0, 1), (-1/2, 1) \end{matrix} \right] \quad (33)$$

In Eq. 33,  $\text{Fo}_{x,\alpha}$  is the ratio between the time  $t$  and the modified diffusion time  $(rc_\alpha x^2)^{1/\alpha}$  associated with the distance  $x$ . For  $\alpha = 1$ , Eq. 33 reduces to:

$$v(x, t) = r_0 i_0 x \left[ -\text{erfc} \left( \frac{1}{\sqrt{4\text{Fo}_x}} \right) + \frac{\sqrt{4\text{Fo}_x}}{\sqrt{\pi}} \exp \left( \frac{-1}{4\text{Fo}_x} \right) \right] \quad (34)$$

Those results correspond to the case of a semi-infinite  $RC$ -based TL.

The current  $i(x, t)$  along the TL can be obtained from the gradient of the voltage via:

$$i(x, t) = -\frac{1}{r} \frac{\partial v(x, t)}{\partial x} \quad (35)$$

which gives:

$$i(x, t) = \frac{2r_0 i_0}{rL} \times \sum_{k=1}^{\infty} \frac{\sin(k\pi x/L)}{k\pi/L} H_{1,2}^{1,1} \left[ \frac{(k\pi/L)^2 t^\alpha}{rc_\alpha} \middle| \begin{matrix} (1, 1) \\ (1, 1), (0, \alpha) \end{matrix} \right] \quad (36)$$

### C. Derivation of impedance function

The impedance of the electrode/electrolyte system is computed from the ratio of the Laplace transform of the voltage by that of the current at the surface  $x = 0$  [14, 15], i.e.:

$$Z_{\text{TL}}(s) = \frac{\mathcal{L}[v(x=0, t); s]}{i_0/s} \quad (37)$$

With the use of the LT formula for an  $H$ -function:

$$\begin{aligned} \mathcal{L} \left[ t^{\rho-1} H_{p,q}^{m,n} \left[ at^\sigma \middle| \begin{matrix} (a_p, A_p) \\ (b_q, B_q) \end{matrix} \right]; t \right] \\ = u^{-\rho} H_{p+1,q}^{m,n+1} \left[ au^{-\sigma} \middle| \begin{matrix} (1-\rho, \sigma), (a_1, A_1), \dots, (a_p, A_p) \\ (b_1, B_1), \dots, (b_q, B_q) \end{matrix} \right] \end{aligned} \quad (38)$$

we obtain

$$\tilde{v}(x=0, s) = \frac{r_0 i_0}{rc_\alpha L} s^{-(1+\alpha)} + \frac{2r_0 i_0}{rc_\alpha L} \sum_{k=1}^{\infty} \frac{1}{s^\alpha + \frac{(k\pi/L)^2}{rc_\alpha}} \quad (39)$$

And knowing that  $\coth(z)$  can be expressed by the series representation:

$$\coth(z) = \frac{1}{z} + 2z \sum_{k=1}^{\infty} \frac{1}{z^2 + (k\pi)^2} \quad (40)$$

the definition given by Eq. 37 leads to the reduced impedance as:

$$\frac{Z_{\text{TL}}(s)}{r_0 L} = \frac{\coth(\sqrt{L^2 rc_\alpha s^\alpha})}{\sqrt{L^2 rc_\alpha s^\alpha}} \quad (41)$$

This is clearly a direct generalization of the case of  $RC$ -based TL with  $\alpha = 1$  [1, 14]. Taking the normalized angular frequency  $s_n = (L^2 rc_\alpha)^{1/\alpha} s$ , we rewrite the impedance function in the form:

$$\frac{Z_{\text{TL}}(s_n)}{r_0 L} = s_n^{-\alpha/2} \coth(s_n^{\alpha/2}) \quad (42)$$

Furthermore, we can proceed by applying one round of inverse Laplace transform using the formula for the  $H$ -function [32]:

$$\begin{aligned} \mathcal{L}^{-1} \left[ u^{-\rho} H_{p,q}^{m,n} \left[ au^\sigma \middle| \begin{matrix} (a_p, A_p) \\ (b_q, B_q) \end{matrix} \right]; t \right] \\ = t^{\rho-1} H_{p+1,q}^{m,n} \left[ at^{-\sigma} \middle| \begin{matrix} (a_p, A_p), \dots, (a_1, A_1), (\rho, \sigma) \\ (b_1, B_1), \dots, (b_q, B_q) \end{matrix} \right] \end{aligned} \quad (43)$$

or that of the Mittag-Leffler (Eq. 19) to find the inverse Laplace transform of  $Z_{\text{TL}}(s)$  (given in Eq. 41) as

$$\begin{aligned} \mathcal{L}^{-1} \{ Z_{\text{TL}}(s); t \} \\ = \frac{r_0 t^{\alpha-1}}{rc_\alpha L \Gamma(\alpha)} \\ + \frac{2r_0}{L} \sum_{k=1}^{\infty} \frac{t^{-1}}{(k\pi/L)^2} H_{2,1}^{1,1} \left[ \frac{(k\pi/L)^2 t^\alpha}{rc_\alpha} \middle| \begin{matrix} (1, 1), (0, -\alpha) \\ (1, 1) \end{matrix} \right] \\ = \frac{r_0 t^{\alpha-1}}{rc_\alpha L \Gamma(\alpha)} + \frac{2r_0}{rc_\alpha L} \sum_{k=1}^{\infty} t^{\alpha-1} E_{\alpha,\alpha} \left( -\frac{(k\pi/L)^2 t^\alpha}{rc_\alpha} \right) \end{aligned} \quad (44)$$

The same result can be found from:

$$\mathcal{L}^{-1} \left\{ \frac{\mathcal{L}[v(x=0, t); s]}{i_0/s}; t \right\} = \frac{1}{i_0} \frac{dv(x=0, t)}{dt} \quad (46)$$

This corresponds to the TL system's response to a step function commonly obtained in experimental chronopotentiometric experiments. We verify that for  $\alpha = 1$ , we obtain from either of the equations (Eqs 44 and 45):

$$\mathcal{L}^{-1} \{ Z_{\text{TL}}(s); t \} = \frac{r_0}{rc_\alpha L} \vartheta_3 \left[ 0, \exp \left( -\frac{\pi^2 t}{rc_\alpha L^2} \right) \right] \quad (47)$$

where  $\vartheta_3(z, q)$  is the Jacobi elliptic theta function defined as [35]:

$$\vartheta_3(z, q) = 1 + 2 \sum_{k=1}^{\infty} q^{k^2} \cos(2kz) \quad (48)$$

By applying another round of inverse Laplace transform (of the  $H$ -function using Eq. 43) following the procedure shown in [36], we obtain the distribution function of relaxation times following the Debye  $RC$  process,  $((1+s\tau)^{-1})$ , as [36]:

$$\begin{aligned} g(\tau) = \frac{\tau^{\alpha-1} \sin(\pi\alpha)}{\pi rc_\alpha L^2} \\ + 2 \sum_{k=1}^{\infty} \frac{\tau^{-1}}{(k\pi)^2} H_{3,1}^{1,1} \left[ \frac{(k\pi/L)^2 \tau^\alpha}{rc_\alpha} \middle| \begin{matrix} (1, 1), (0, -\alpha), (1, \alpha) \\ (1, 1) \end{matrix} \right] \end{aligned} \quad (49)$$

This means that  $Z_{\text{TL}}(s)/(r_0L) = \int_0^\infty g(\tau)(1+s\tau)^{-1}d\tau$ . We can also have from the inverse Laplace transform of the Mittag-Leffler function using formula 92 in [37]:

$$x^{1-1/\alpha}E_{\alpha,\alpha}(-x) = \frac{\sin(\alpha\pi)}{\pi} \int_0^\infty \frac{u^\alpha e^{-x^{1/\alpha}u}}{1+2u^\alpha \cos(\alpha\pi) + u^{2\alpha}} du \quad (50)$$

the following expression for  $g(\tau)$ :

$$g(\tau) = \frac{\sin(\pi\alpha)}{\pi r c_\alpha L^2} \times \left( \tau^{\alpha-1} + 2 \sum_{k=1}^\infty \frac{\tau^{-\alpha-1}}{\tau^{-2\alpha} + 2b_k \tau^{-\alpha} \cos(\alpha\pi) + b_k^2} \right) \quad (51)$$

where  $b_k = (k\pi)^2/(rc_\alpha L^2)$ , and  $0 < \alpha < 1$ .

### III. RESULTS AND DISCUSSION

With a normalizing voltage of  $i_0 r_0 L$ , a dimensionless time  $t_n = t/(rc_\alpha L^2)^{1/\alpha}$  [15] and  $x_n = x/L$ , the voltage initially given by Eq. 26 is rewritten as:

$$\begin{aligned} v_n(x_n, t_n) &= \frac{t_n^\alpha}{\Gamma(1+\alpha)} \\ &+ 2 \sum_{k=1}^\infty \frac{\cos(k\pi x_n)}{(k\pi)^2} H_{1,2}^{1,1} \left[ (k\pi)^2 t_n^\alpha \left| \begin{matrix} (1, 1) \\ (1, 1), (0, \alpha) \end{matrix} \right. \right] \\ &= \frac{t_n^\alpha}{\Gamma(1+\alpha)} + 2 \sum_{k=1}^\infty \cos(k\pi x_n) t_n^\alpha E_{\alpha,\alpha+1} \left( -(k\pi)^2 t_n^\alpha \right) \end{aligned} \quad (52) \quad (53)$$

Numerical simulations of this function for the positions  $x_n = x/L = 0, 0.5, 1.0$  on the TL and for  $\alpha = 1.0, 0.75, 0.5$  are given in Fig. 3. The infinite sum is truncated to its first 10 terms. We note that Posey and Morozumi [27] reported the same results for  $\alpha = 1$  (Fig. 3(a)). On the second  $y$ -axis, we show plots of the Caputo time derivative of  $v_n(x_n, t_n)$ , i.e.:

$${}_0D_{t_n}^\alpha v_n(x_n, t_n) = 1 + 2 \sum_{k=1}^\infty \cos(k\pi x_n) E_\alpha \left( -(k\pi)^2 t_n^\alpha \right) \quad (54)$$

which indicates saturation of the current on the CPE as time increases.

Plots of the impedance function given by Eq. 42 are presented in Fig. 4 for values of  $\alpha$  between 1.0 and 0.5. The frequency range covered for the normalized angular frequency  $\omega_n$  ( $s_n = i\omega_n$ ) is  $\pi/10$  to  $200\pi$ . The impedance plots are shown in terms of magnitude vs. frequency (Fig. 4(a)), phase vs. frequency (Fig. 4(b)), and (negative) imaginary vs. real part of the function (Fig. 4(c)). As discussed above, the impedance function shows clearly

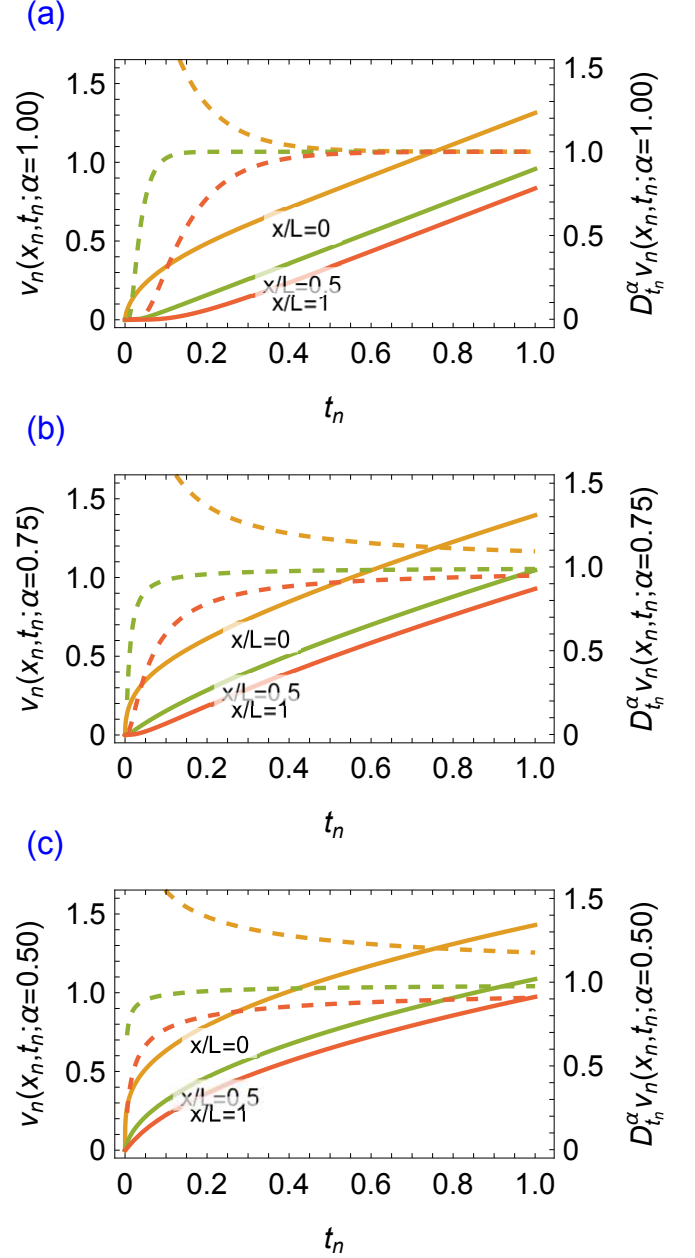


FIG. 3. Plot of voltage  $v_n(x_n, t_n)$  given by Eq. 53 (for galvanostatic charging of an  $R$ -CPE TL circuit on a bounded domain  $[0; L]$ ) vs.  $t_n = t/(rc_\alpha L^2)^{1/\alpha}$  for  $x/L = 0, 0.5, 1.0$  and for (a)  $\alpha = 1.0$ , (b)  $\alpha = 0.75$  and (c)  $\alpha = 0.5$

two separate regimes when looking at the Nyquist complex plots in Fig. 4(c). For  $s_n \rightarrow 0$ , the leading order of Eq. 42 is  $1/3 + s_n^{-\alpha}$ , which is marked in the figure by dashed straight lines for the different values of  $\alpha$ . These lines form angles of  $\alpha\pi/2$  with the real axis, and all intersect at the real axis at  $\text{Re}(Z_{\text{TL}}/r_0L) = 1/3$ . For the ideal case, we have a vertical line as it should be [25], which indicates pure capacitive behavior. Whereas at high frequencies, the impedance tends to  $s_n^{-\alpha/2}$ , which

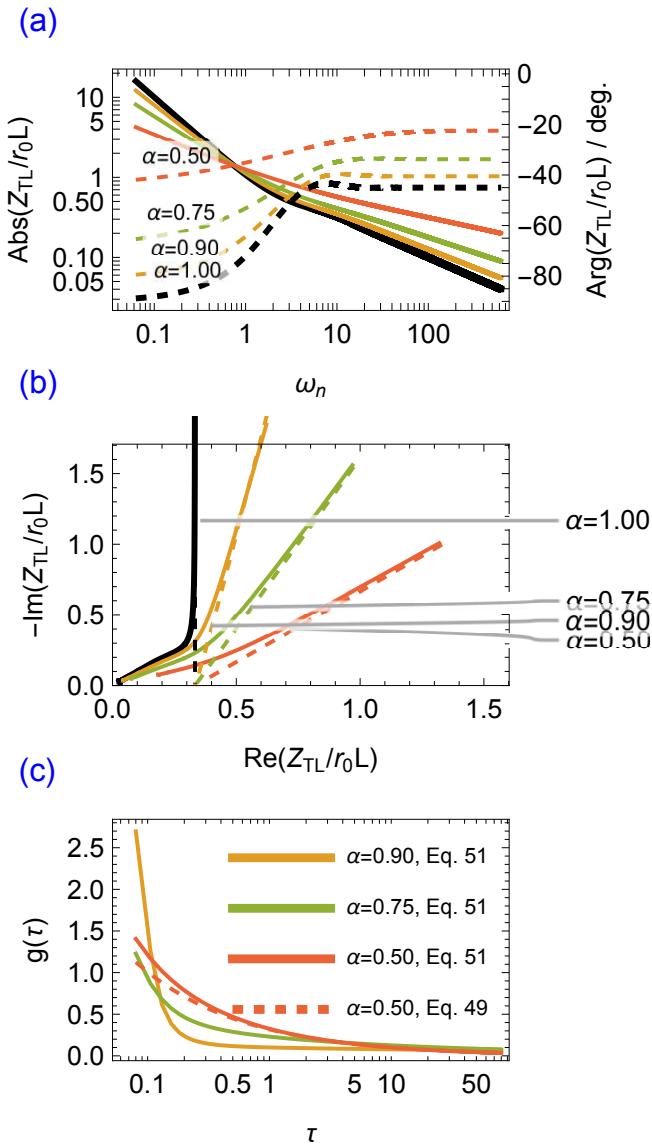


FIG. 4. Plot of impedance function given by Eq. 42 for different values of  $\alpha$  in terms of (a) magnitude vs. frequency (solid lines), and phase vs. frequency (dashed lines), and (b) imaginary vs. real part of impedance (dashed lines represent  $1/3 + s_n^{-\alpha}$  at the limit of  $s_n \rightarrow 0$ ). In (c) we show plots of the associated distribution function of relaxation times  $g(\tau)$  (Eqs. 49 and 51) vs  $\tau$

corresponds to lines inclined from the real axis with half the inclination angle observed for the low frequency data ( $\alpha\pi/4$ ). For  $\alpha = 1$ , we obtain the classical case of 45 deg. inclined Warburg element for semi-infinite linear diffusion.

Finally, we show in Fig. 4(c) simulation plots of both derived distribution functions of relaxation time  $g(\tau)$  (i.e. Eqs. 49 and 51, up to the first 10 terms of the summation) vs.  $\tau$ , for  $\alpha = 0.5$ . The time parameter ( $rc_\alpha L^2$ ) is set to one. The two expressions show some deviation from each other for very small values of  $\tau$ , otherwise, they are in good agreement overall. We also plot Eq. 51 for the  $\alpha$ -values of 0.90 and 0.75. It is clear that the distribution of relaxation times, as it should be, is narrower as  $\alpha$  is increased toward one, and vice versa it gets wider as  $\alpha$  is decreased.

#### IV. CONCLUSION

In this work, we showed that the modified impedance model  $s_n^{-\alpha/2} \coth(s_n^{\alpha/2})$  obtained empirically by inserting the dispersion coefficient  $\alpha$  into the classical theory  $s_n^{-1/2} \coth(s_n^{1/2})$  that describes bounded diffusion, can be derived exactly from the (Caputo) time-fractional diffusion equation (Eq. 8). This corresponds to a homogeneous TL model consisting of distributed  $R$ s with CPEs of constant parameters. Importantly, we also derived by inverse Laplace transform the system's response to a step function (Eq. 44 or 45), and by another inverse Laplace transform the distribution function of relaxation times of the Debye type (Eqs. 49 or 51). These formulas are provided in terms of the Fox's  $H$ -function and in terms of the Mittag-Leffler function, which are functions frequently encountered in fractional calculus. The results of this study can find many practical applications for the fundamental analysis of electrochemical systems in the time and frequency domains, as well as other mass or heat problems obeying Eq. 8.

#### ACKNOWLEDGEMENTS

C.W. acknowledges the funding support by the National Science Foundation, awards #2423124 and #2412500.

- [1] J. Bisquert and A. Compte, Theory of the electrochemical impedance of anomalous diffusion, . *Electroanal. Chem.* **499**, 112 (2001).
- [2] J. Bisquert, G. Garcia-Belmonte, F. Fabregat-Santiago, N. S. Ferriols, P. Bogdanoff, and E. C. Pereira, Doubling exponent models for the analysis of porous film electrodes by impedance. relaxation of tio2 nanoporous in aqueous

- solution, *J. Phys. Chem. B* **104**, 2287 (2000).
- [3] J. Song and M. Z. Bazant, Electrochemical impedance imaging via the distribution of diffusion times, *Phys. Rev. Lett.* **120**, 116001 (2018).
- [4] A. A. Moya, Low-frequency approximations to the finite-length warburg diffusion impedance: The reflexive case, *J. Energy Storage* **97**, 112911 (2024).

- [5] D. R. Franceschetti and J. R. Macdonald, Diffusion of neutral and charged species under small-signal ac conditions, *J. Electroanal. Chem. Interfacial Electrochem.* **101**, 307 (1979).
- [6] C. Gabrielli, O. Haas, and H. Takenouti, Impedance analysis of electrodes modified with a reversible redox polymer film, *J. Appl. Electrochem.* **17**, 82 (1987).
- [7] J. Farcy, R. Messina, and J. Perichon, Kinetic study of the lithium electroinsertion in  $\text{V}_2\text{O}_5$  by impedance spectroscopy, *J. Electrochem. Soc.* **137**, 1337 (1990).
- [8] C. Ho, I. Raistrick, and R. Huggins, Application of a-c techniques to the study of lithium diffusion in tungsten trioxide thin films, *J. Electrochem. Soc.* **127**, 343 (1980).
- [9] J. H. Xu, T. Schoetz, J. R. McManus, V. R. Subramanian, P. W. Fields, and R. J. Messinger, Tunable pseudocapacitive intercalation of chloroaluminate anions into graphite electrodes for rechargeable aluminum batteries, *J. Electrochem. Soc.* **168**, 060514 (2021).
- [10] D. Ohayon, G. Quek, B. R. P. Yip, F. Lopez-Garcia, P. R. Ng, R. J. Vázquez, D. V. Andreeva, X. Wang, and G. C. Bazan, High-performance aqueous supercapacitors based on a self-doped n-type conducting polymer, *Adv. Mater.* , 2410512 (2024).
- [11] R. Cabanel, G. Barral, J. P. Diard, B. Le Gorrec, and C. Montella, Determination of the diffusion coefficient of an inserted species by impedance spectroscopy: application to the  $\text{H}^+/\text{H}_x\text{Nb}_2\text{O}_5$  system, *J. Appl. Electrochem.* **23**, 93 (1993).
- [12] I. Profatilova, E. De Vito, S. Genies, C. Vincens, E. Gutel, O. Fanget, A. Martin, M. Chandesris, M. Tulodziecki, and W. Porcher, Impact of silicon/graphite composite electrode porosity on the cycle life of 18650 lithium-ion cell, *ACS Appl. Energy Mater.* **3**, 11873 (2020).
- [13] R. De Levie, On porous electrodes in electrolyte solutions: I. capacitance effects, *Electrochim. Acta* **8**, 751 (1963).
- [14] C. Pedersen, T. Aslyamov, and M. Janssen, Equivalent circuit and continuum modeling of the impedance of electrolyte-filled pores, *PRX Energy* **2**, 043006 (2023).
- [15] A. Allagui and E. H. Balaguera, On the semi-infinite distributed resistor-constant phase element transmission line, *Electrochim. Acta* , 145344 (2024).
- [16] A. C. Lazanas and M. I. Prodromidis, Electrochemical impedance spectroscopy—a tutorial, *ACS Meas. Sci. Au* **3**, 162 (2023).
- [17] A. Allagui and A. S. Elwakil, Tikhonov regularization for the deconvolution of capacitance from voltage-charge response of electrochemical capacitors, *Electrochim. Acta* , 142527 (2023).
- [18] A. Allagui and H. Benaoum, Power-law charge relaxation of inhomogeneous porous capacitive electrodes, *J. Electrochem. Soc.* **169**, 040509 (2022).
- [19] A. Allagui and A. S. Elwakil, Possibility of information encoding/decoding using the memory effect in fractional-order capacitive devices, *Sci. Rep.* **11**, 1 (2021).
- [20] A. Allagui and M. E. Fouda, Inverse problem of reconstructing the capacitance of electric double-layer capacitors, *Electrochim. Acta* , 138848 (2021).
- [21] A. Allagui, A. S. Elwakil, and C. Psychalinos, Decoupling the magnitude and phase in a constant phase element, *J. Electroanal. Chem.* **888**, 115153 (2021).
- [22] J. Huang, Diffusion impedance of electroactive materials, electrolytic solutions and porous electrodes: Warburg impedance and beyond, *Electrochim. Acta* **281**, 170 (2018).
- [23] M. Janssen, Transmission line circuit and equation for an electrolyte-filled pore of finite length, *Phys. Rev. Lett.* **126**, 136002 (2021).
- [24] A. Gupta, P. J. Zuk, and H. A. Stone, Charging dynamics of overlapping double layers in a cylindrical nanopore, *Phys. Rev. Lett.* **125**, 076001 (2020).
- [25] M. Janssen and J. Bisquert, Locating the frequency of turnover in thin-film diffusion impedance, *J. Phys. Chem. B* **125**, 15737 (2021).
- [26] O. P. Agrawal, Solution for a fractional diffusion-wave equation defined in a bounded domain, *Nonlinear Dynamics* **29**, 145 (2002).
- [27] F. Posey and T. Morozumi, Theory of potentiostatic and galvanostatic charging of the double layer in porous electrodes, *J. Electrochem. Soc.* **113**, 176 (1966).
- [28] A. G. Strandhagen, Use of sine transform for non-simply supported beams, *Q. Appl. Math.* **1**, 346 (1944).
- [29] I. Roettinger, A generalization of the finite fourier transformation and applications, *Q. Appl. Math.* **5**, 298 (1947).
- [30] K. Al-Khaled, Finite fourier transform for solving potential and steady-state temperature problems, *Adv. Differ. Equations* **2018**, 1 (2018).
- [31] T. R. Prabhakar, A singular integral equation with a generalized mittag leffler function in the kernel, *Yokohama Math. J.* **19**, 7 (1971).
- [32] A. M. Mathai, R. K. Saxena, and H. J. Haubold, *The H-function: theory and applications* (Springer Science & Business Media, 2009).
- [33] Y. Luchko, Initial-boundary-value problems for the one-dimensional time-fractional diffusion equation, *Fract. Calc. Appl. Anal.* **15**, 141 (2012).
- [34] Y. Luchko, Some uniqueness and existence results for the initial-boundary-value problems for the generalized time-fractional diffusion equation, *Comput. Math. Appl.* **59**, 1766 (2010).
- [35] Mathematica, <https://functions.wolfram.com/introductions/pdf/ellip>
- [36] A. Allagui and A. S. Elwakil, Procedure for obtaining the analytical distribution function of relaxation times for the analysis of impedance spectra using the fox h-function, *J. Phys. Chem. C* **128**, 2788 (2024).
- [37] P. Van Mieghem, The mittag-leffler function, arXiv preprint arXiv:2005.13330 (2020).